SUPPLEMENTARY MATERIALS

Ferroelectricity in bis(ethylammonium) pentachlorobismuthate(III); synthesis, structure, polar and spectroscopic properties

Anna Piecha-Bisiorek[a*], Anna Gągor[b], Ryszard Jakubas[a], Agnieszka Ciżman[c], Rafał Janicki[a] and Wojciech Medycki[d]

[a]Faculty of Chemistry, University of Wrocław, F. Joliot-Curie 14, 50-383 Wrocław, Poland. E-mail: anna.piecha@chem.uni.wroc.pl.

[b]W. Trzebiatowski Institute of Low Temperature and Structure Research PAS, P.O. Box 1410, 50-950 Wrocław, Poland.

[c]Institute of Physics, Wrocław University of Technology, Wybrzeże Wyspiańskiego 27, Wrocław, Poland.

[d]Institute of Molecular Physics, Polish Academy of Science, Smoluchowskiego 17, 60-179 Poznań, Poland.

TABLE OF CONTENS:

Part 1

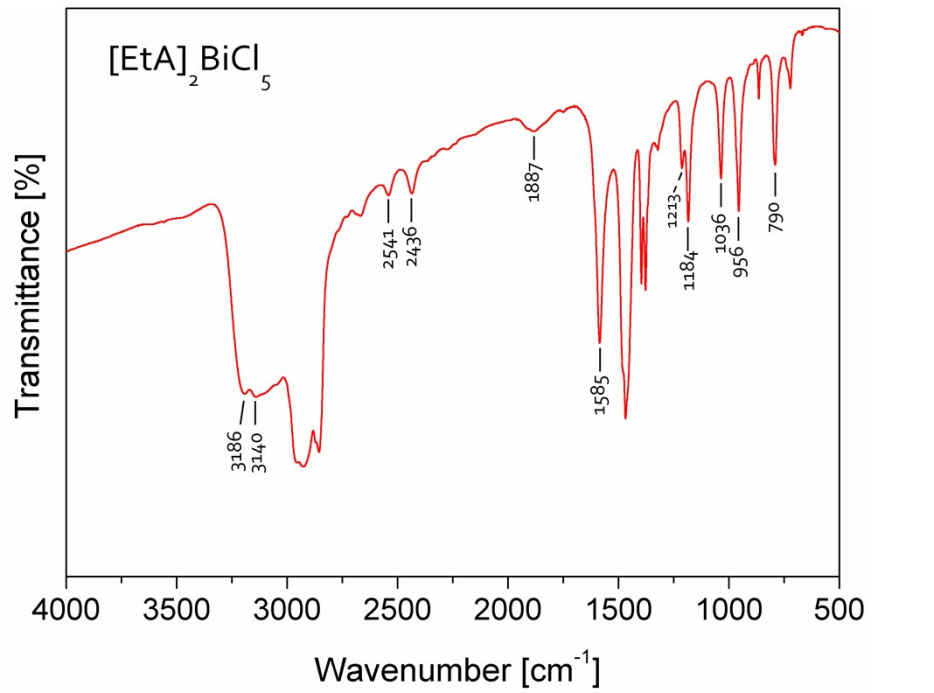

Figure S1. The infrared spectrum of the powdered **ECB** sample in Nujol at 295 K.

Part 2

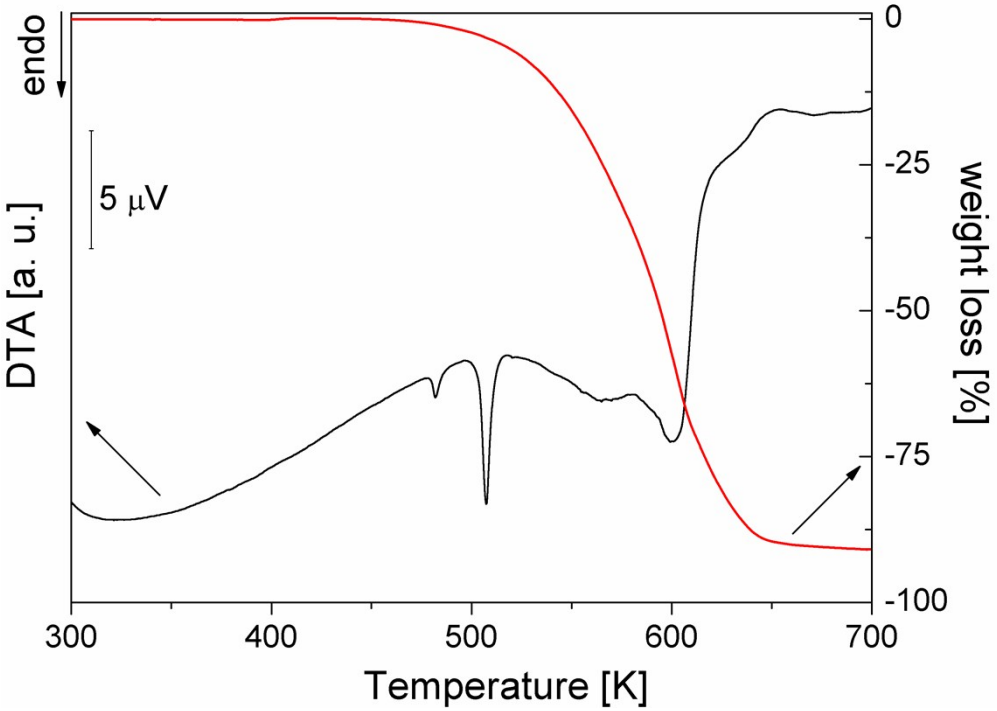

Figure S2. TGA and DTA scans for **ECB**.

Part 3

Table S1. Experimental details

For all structures: $C_4H_{16}BiCl_5N_2$, M_r = 478.42, Z = 8. Experiments were carried out with Mo$K\alpha$ radiation. H-atom parameters were constrained.

	Phase I	**Phase II**
Crystal data		
Crystal system, space group	Orthorhombic, *Acam*	Orthorhombic, *Aba*2
Temperature (K)	295	100
a, *b*, *c* (Å)	17.8318 (2), 21.9673 (8), 7.5656 (4)	17.5405 (4), 21.7670 (4), 7.4791 (2)
V (Å^3)	2963.57 (19)	2855.54 (10)
μ (mm^{-1})	12.76	13.25
Crystal size (mm)	0.21 × 0.18 × 0.15	0.21 × 0.16 × 0.10
Data collection		
T_{min}, T_{max}	0.301, 1.000	0.193, 1.000
No. of measured, independent and observed [$I > 2\sigma(I)$] reflections	32217, 2229, 1917	11801, 2869, 2687
R_{int}	0.043	0.060
$(\sin \theta/\lambda)_{max}$ (Å^{-1})	0.694	0.694
Refinement		
$R[F^2 > 2\sigma(F^2)]$, $wR(F^2)$, S	0.027, 0.069, 1.12	0.039, 0.111, 1.11
No. of reflections	2229	2869
No. of parameters	78	137
No. of restraints	34	40
$\Delta\rho_{max}$, $\Delta\rho_{min}$ (e Å^{-3})	0.86, -0.74	1.68, -2.17
Absolute structure	–	Refined as an inversion twin.
Absolute structure parameter	–	0.462 (17)

Computer programs: *CrysAlis PRO*, Agilent Technologies, Version 1.171.37.35h (release 09-02-2015 CrysAlis171 .NET) (compiled Feb 9 2015, 16:26:32), *CrysAlis CCD*, Oxford Diffraction Ltd., Version 1.171.33.66 (release 28-04-2010 CrysAlis171 .NET) (compiled Apr 28 2010, 14:27:37), *CrysAlis RED*, *SHELXL2014/7* (Sheldrick, 2014).

Table S2 Selected geometric parameters (Å, º)

RT (Phase I)		**100 K (Phase II)**	
Bi1—Cl1^{i}	2.5771 (13)	Bi1—Cl11	2.532 (3)
Bi1—Cl1	2.5771 (13)	Bi1—Cl1	2.598 (3)
Bi1—Cl2	2.676(1)	Bi1—Cl2	2.682 (3)
Bi1—Cl3	2.688 (2)	Bi1—Cl3	2.717 (3)
Bi1—Cl4^{i}	2.8408 (6)	Bi1—Cl4	2.834 (3)
Bi1—Cl4	2.8408 (6)	Bi1—Cl4^{iii}	2.934 (3)
Cl1^{i}—Bi1—Cl1	95.32 (8)	Cl11—Bi1—Cl1	95.08 (10)
Cl1^{i}—Bi1—Cl2	87.91 (5)	Cl11—Bi1—Cl2	90.50 (9)
Cl1—Bi1—Cl2	87.91 (5)	Cl1—Bi1—Cl2	86.24 (11)
Cl1^{i}—Bi1—Cl3	91.72 (5)	Cl11—Bi1—Cl3	90.17 (10)
Cl1—Bi1—Cl3	91.72 (5)	Cl1—Bi1—Cl3	91.00 (13)
Cl2—Bi1—Cl3	179.45 (7)	Cl2—Bi1—Cl3	177.21 (12)
Cl1^{i}—Bi1—Cl4^{i}	174.07 (4)	Cl11—Bi1—Cl4	85.90 (10)

Cl1—Bi1—Cl4^{i}	90.60 (4)	Cl1—Bi1—Cl4	179.02 (10)
Cl2—Bi1—Cl4^{i}	91.92 (8)	Cl2—Bi1—Cl4	93.64 (8)
Cl3—Bi1—Cl4^{i}	88.50 (8)	Cl3—Bi1—Cl4	89.12 (11)
Cl1^{i}—Bi1—Cl4	90.60 (4)	Cl11—Bi1—Cl4^{iii}	168.92 (10)
Cl1—Bi1—Cl4	174.07 (4)	Cl1—Bi1—Cl4^{iii}	95.92 (10)
Cl2—Bi1—Cl4	91.91 (8)	Cl2—Bi1—Cl4^{iii}	88.92 (8)
Cl3—Bi1—Cl4	88.50 (8)	Cl3—Bi1—Cl4^{iii}	90.95 (9)
Cl4^{i}—Bi1—Cl4	83.49 (2)	Cl4—Bi1—Cl4^{iii}	83.10 (3)
Bi1—Cl4—Bi1^{ii}	162.82 (14)	Bi1—Cl4—Bi1^{iv}	148.76 (11)

Symmetry code(s): (i) *x*, *y*, -*z*; (ii) -*x*+3/2, *y*, -*z*-1/2; (iii) -*x*+3/2, *y*, *z*+1/2; (iv) -*x*+3/2, *y*, *z*-1/2.

Table S3 Selected hydrogen-bond parameters

D*—H···*A	***D*—H (Å)**	**H···*A* (Å)**	***D*···*A* (Å)**	***D*—H···*A* (°)**
RT				
N1B—H6···Cl3^{i}	0.89	2.55	3.250 (7)	136
N1B—H3···Cl1^{ii}	0.89	2.48	3.367 (6)	172
N1A—H13···Cl1^{iv}	0.89	2.60	3.416 (8)	153
N1A—H10···Cl2	0.89	2.71	3.343 (12)	130
100 K				
N1A—H1···Cl2	0.89	2.43	3.303 (11)	165.7
N1A—H2···Cl2^{vi}	0.89	2.44	3.307 (9)	165.7
N1A—H3···Cl4^{vii}	0.89	2.48	3.323 (10)	157.7
N1B—H9···Cl3^{viii}	0.89	2.53	3.41 (3)	171.1
N1B—H10···Cl1^{iii}	0.89	2.30	3.11 (2)	150.2
N1B—H11···Cl3^{i}	0.89	2.41	3.25 (2)	157.0
N2B—H17···Cl3^{i}	0.89	2.32	3.18 (4)	163.3
N2B—H18···Cl3^{viii}	0.89	2.24	3.06 (4)	153.0
N2B—H19···Cl1^{iii}	0.89	2.59	3.46 (4)	168.6

Symmetry code(s): (i) *x*-1/2, -*y*, *z*+1/2; (ii) -*x*+1, -*y*, -*z*+1; (iii) -*x*+1, -*y*, *z*; (iv) -*x*+1, -*y*+1/2, *z*-1/2; (v) *x*, *y*, -*z*; (vi) -*x*+1, -*y*+1/2, *z*+1/2; (vii) *x*, *y*, *z*+1; (viii) -*x*+1, -*y*, *z*+1.

3.1 Amplimodes analysis

WP		Atom	Atomic Displacements			
			u_x	u_y	u_z	|u|
8b	(x,y,z)	Bi1	-0.0006	0.0009	-0.0031	0.0328
8b	(x,y,z)	Cl1	0.0107	-0.0067	0.0231	0.2978
8b	(x,y,z)	Cl1_2	-0.0113	-0.0009	0.0237	0.2707
8b	(x,y,z)	Cl2	-0.0047	0.0006	0.0401	0.3150
8b	(x,y,z)	Cl3	0.0020	-0.0008	-0.0314	0.2407
8b	(x,y,z)	Cl4	0.0231	0.0070	-0.0524	0.5920

NOTE: u_x, u_y and u_z are given in relative units. |u| is the absolute distance
Maximum atomic displacement in the distortion, Δ: 0.5920 Å
Total distortion amplitude: 1.6379 Å

Symmetry Modes Summary

Atoms	WP	Modes
Cl1	16*g*	GM1+(3) **GM3-(3)**
Cl3 Bi1 Cl2	8*f*	GM1+(2) **GM3-(1)**
Cl4	8*e*	GM1+(1) **GM3-(2)**

Note: The primary mode is written in bold letters

Summary of Amplitudes

K-vector	Irrep	Direction	Isotropy Subgroup	Dimension	Amplitude (Å)
(0,0,0)	GM1+	(a)	Cmca (64)	10	0.4051
(0,0,0)	GM3-	(a)	Aba2 (41)	8	1.5869

Global distortion: 1.6378 Å

Part 4. Dielectric properties

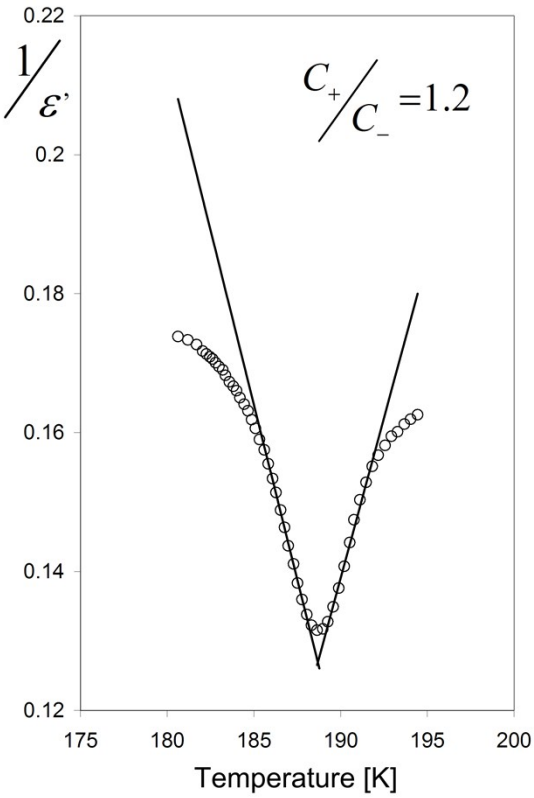

Figure S3. TGA and DTA scans for $[EtA]_2BiCl_5$.

The electrical response can be analyzed through complex electric modulus formalism. The complex electric modulus, M^* is defined as:

$$M^* = M' + iM'' = \frac{1}{\varepsilon^*} = \frac{\varepsilon'}{\varepsilon'^2 + \varepsilon''^2} + \frac{i\varepsilon''}{\varepsilon'^2 + \varepsilon''^2},$$

where M', M'' denote the real and the imaginary parts of dielectric modulus, and ε′ and ε″ are the real and the imaginary parts of the dielectric permittivity, respectively [1]. The frequency dependence of the imaginary part of the electrical modulus $M''(\omega)$ at various temperatures is shown in Fig. S5.

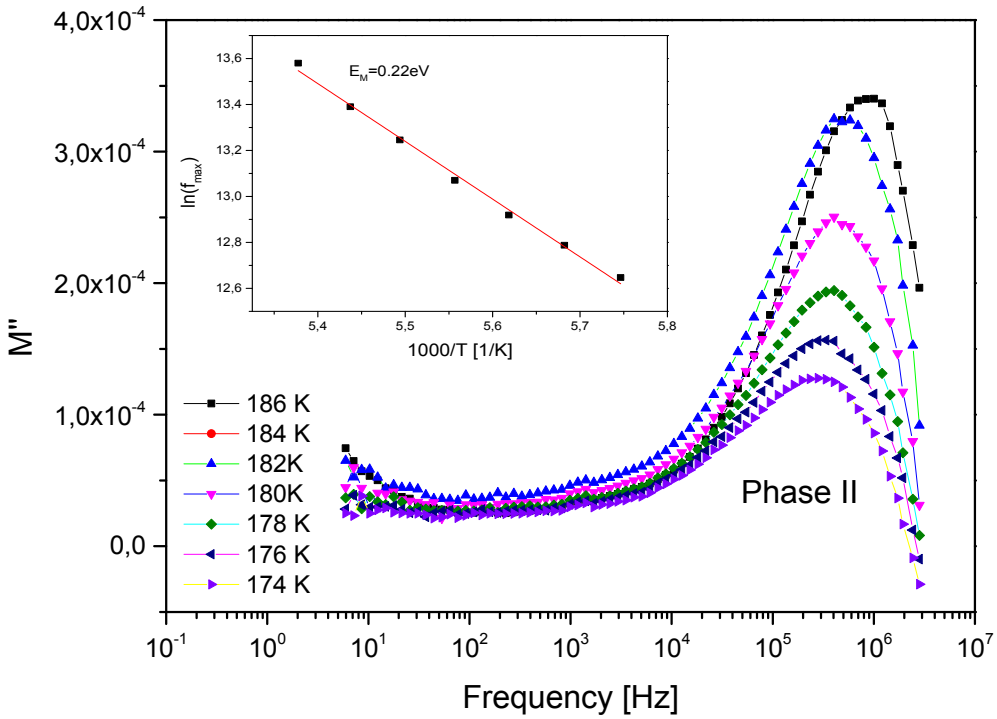

Figure S4. Variation of imaginary part of electric modulus with frequency for different temperatures. The data are connected as a guide to the eye. Insert shows the frequency dependences of the M'' peak on 1000/T . Line represents a fit to the Arrhenius expression.

The peak maxima position shifts toward higher frequencies with rising temperature, while a shape of the curves is asymmetric, exhibiting non-Debye behaviour in a high frequency region. The asymmetric modulus peaks shifts towards higher frequency side can be attributed to the correlation between the motions of mobile charge carriers [2]. To get further insight into the dynamics of the relaxation process, the measuring frequency ($\ln f_{max}$) vs temperature (1000/T) of the peak maximum in an Arrhenius-type representation was plotted (Insert in Figure S5). The dots are the experimental data and the solid line represents the least-squares straight-line fit of the relaxation of M''(ω). Assuming, the relaxation process around 180 K with the relaxation energy about E_M = 0.22eV can be attributed, most probably with the domain wall motion.

[1] A. K. Jonscher, M. S. Frost, *Thin Solid Films*, 1976, **37**, 267-273.
[2] T. Kobayashi, Y. Noguchi, M. Miyayama, *Appl. Phys. Lett.*, 2005, **86**, 012907-1-3.

Part 5. Proton magnetic resonance studies (^{1}H NMR)

If relaxation is predominantly due to dipolar interactions modulated by non-correlated reorientational motions of several inequivalent proton groups, the spin–lattice relaxation rate can be described by the well established formula [3]:

$$\frac{1}{T_1} = \sum_{i=1}^{n} C_i \left[\frac{\tau_{ci}}{1+\omega^2\tau_{ci}^2} + \frac{4\tau_{ci}}{1+4\omega^2\tau_{ci}^2} \right] \quad \text{(S1)}$$

where τ_{ci} is the correlation time of the motion involved in the relaxation process according to the Arrhenius law($\tau_c = \tau_0 \exp(E_a/RT)$, where τ_0 is the correlation time at the limit infinite temperature, E_a – the height of the barrier, R – gas constant), ω - the Larmor angular frequency, and C_i is the dipolar relaxation constant. It is readily seen that two different relaxation processes are observed in the **ECB** compound. When we take n=2 then we obtain theoretical curve well fitted to the points of both different slopes and both temperature minima. The theoretical values of the E_a and τ_o estimated from the fitting procedure using Eq. (1) are shown in Table 5. In fact the ethylammonium cation possesses to three-proton groups, namely CH_3 and NH_3 which may relax independently forming two different spin-lattice relaxation time neighboring minima [4]. But due to the difference between distances H-H in both three-proton groups the obtained relaxation constants $C_{1,2}$ should be more different as 20% and more than the observed about 3%. It is mean that both observed minima are resulting from two inequivalent relaxing ethylammonium cations with the fast spin diffusion inside each cation.

The activation energy values for these reorientations in both cations are typical for three proton groups like CH_3 or NH_3 and comparable values were also found in literature [5].

Just above the phase transition at 190K the estimated activation energy is about 4,57 kcal/mol and then gradually drops to 2.05 kcal/mol. Appearance with increasing of temperature of more available space and vanishing of possible strong hydrogen bonds of NH_3 groups probably leads to the unified axial like motion of whole ethylamine molecule for both cations.

Table S4. Motional parameters obtained from fitting of the theoretical line (eq. S1) to date points for **ECB**.

parameter	Cation A motion	Cation B motion
E_a [kJ/mol]	1.96	2.96
τ_0 [s]	$2.9\ 10^{-13}$	$7.8\ 10^{-14}$
C [s^{-2}]	$3.8\ 10^{9}$	$3.7\ 10^{9}$

[3] N. Bloembergen, E.M. Purcell, R.V. Pound, Phys. Rev. 73, 679-712 (1948)
[4] H. Ishida, N. Kumaga S. Sato Z. Naturforsch. 56a, 523-526 (2001)
[5] H. Terao, Y. Furukawa, M. Hashimoto, K. Yamada, T. Okuda Z. Naturforsch. 57 a, 369–374 (2002)